Supporting Information

Carbonization of Human Fingernails: Toward the Sustainable Production of Multifunctional Nitrogen and Sulfur Codoped Carbon Nanodots with Highly Luminescent Probing and Cell Proliferative/Migration Properties

Theodoros G. Chatzimitakos,[†] Athanasia I. Kasouni,[††] Anastassios N. Troganis,[††] Constantine D. Stalikas*[,†]

[†]*Laboratory of Analytical Chemistry, Department of Chemistry, and* [††]*Laboratory of Biophysical Chemistry, Department of Biological Applications and Technologies, University of Ioannina, 45110, Ioannina, Greece*

*Corresponding author, e-mail: cstalika@cc.uoi.gr

Chemicals

Stock solutions of metal ions (at concentration of 1000 mg L^{-1}) and crystal violet were obtained from Merck (Darmstadt, Germany). Quinine hemisulfate monohydrate was purchased from Alfa Aesar (Karlsruhe, Germany). Potassium chromate, sodium chloride, potassium chloride, fetal bovine serum (FBS), Roswell Park Memorial Institute medium (RPMI-1640), Dulbecco's Modified Eagle's medium (DMEM), antibiotics (50 units mL^{-1} penicillin and 50 µg mL^{-1} streptomycin), phosphate buffer saline (PBS), trypan blue, formaldehyde solution (37% w/v), Ribonuclease type A, trypsin solution 0.05%, 3,5-Di-*tert*-4-butylhydroxytoluene (BHT), 1,1-diphenyl-2-picrylhydrazyl (DPPH) and Triton™X-100 were obtained from Sigma Aldrich (Steinheim, Germany). Propidium iodide staining solution (1.0 mg mL^{-1} in water) was obtained from Biotium (Fremont, California). Double distilled water (DDW) was used throughout the experiments. The solvents used were of HPLC grade. The crystal violet solution used for the estimation of cell number consisted of 0.4% w/v crystal violet, 5 mL of 37% w/v formaldehyde solution, 0.25 g sodium chloride, 50 mL methanol and 45 mL DDW. Trypan blue was diluted in PBS (0.04% w/v). Normal saline was prepared by dissolving 0.9 g of NaCl in 100 mL of DDW.

Instrumentation

FTIR spectra were recorded on a Spectrum Two FTIR using an attenuated total reflectance accessory (PerkinElmer, MA, USA). High resolution-transmission electron microscopy (HR-TEM) images were obtained with a JEOL JEM-2100 microscope operated at 200 kV equipped with LaB6 filament. Samples for HR-TEM measurements were prepared by depositing a drop of CNDs dispersion on carbon-coated copper grids and drying at room temperature. The photoemission experiments were carried out in an ultra-high vacuum system (UHV) which consists of a fast entry specimen assembly, a sample preparation and an analysis chamber. The base pressure in both chambers was 1×10^{-9} mbar. Unmonochromatized MgKα line at 1253.6 eV and an analyzer pass energy of 36 eV, giving a full width at half maximum (FWHM) of 0.9 eV for the Au $4f_{7/2}$ peak, were used in all XPS measurements. The XPS core level spectra were analyzed using a fitting routine, which can decompose each spectrum into individual mixed Gaussian-Lorentzian peaks after a Shirley background subtraction. The samples were in powder form and pressed into pellets (stainless steel). Errors in our quantitative data were found in the range of ~10% (peak areas)

while the accuracy for BEs assignments is ~0.1 eV. All fluorescence measurements were performed on a RF 5301 PC spectrofluorometer (Shimadzu, Japan) with excitation slit set at 5 nm band pass and emission at 5 nm band pass, in a quartz cell of 1×1 cm. The UV-Vis absorption spectra were recorded on a Lambda 35 UV-Vis spectrometer (Perkin Elmer, Germany). Lyophilization of the samples was carried out by an Alpha 1-4 LD freeze-dryer (Christ, Germany) and centrifugation of CNDs suspension by a PrO-Research centrifuge (Centurion, Sci., West Sussex, UK). Digital images for scratch assay and cell imaging were captured with an Infinity 2-2 digital camera (Lumenera, Canada), mounted on an Olympus BX43 microscope, under U-HGLGPS light guide-coupled illumination system. Fluorescent activated cell sorting (FACS) was performed on a FACScan flow cytometer (BD FACS Aria). BD FACS Diva software was used to analyze the resulting DNA histograms using a planimetrie method.

Quantum yield

A standard solution of quinine sulfate dissolved in 0.1 M H_2SO_4 [refractive index (η)=1.33] was chosen as a reference, whose QY is reported to be 54%. Aqueous solutions (η=1.33) of varying concentrations of the CNDs were prepared. The absorbances of the solutions were measured at the excitation wavelength, using a UV-Vis spectrophotometer. Fluorescence emission intensity was recorded for solutions, whose absorption was lower than 0.1 a.u. The QY (Φ_x) for each of the two CNDs were calculated using the following equation:

$$\Phi_x = \Phi_{st} \left(\frac{Slope_x}{Slope_{st}}\right)\left(\frac{n_x^2}{n_{st}^2}\right)$$

where *x* and *st* denote the sample and the quinine sulfate, respectively. Φ is the QY; *slope*, is the slope of the integrated fluorescence emission intensity versus the absorbance and *n* is the refractive index of the solvent.[1]

Cell culture conditions

The A549, MDA-MB-231 and HEK-293 cells were grown in RPMI-1640 supplemented with 1% antibiotics and 10% heat-inactivated FBS, while HeLa cells were grown in DMEM medium. All cell lines were grown in a humidified 5% carbon dioxide atmosphere at 37°C. Cells were maintained in 75 cm^2 flasks by passage every 2 to 3 days.

Cell viability

Cells were seeded into 24-well plates at a density of 7×10^4 cells/well (short term viability assay) or 4×10^4 cell/well (long term viability assay) in 0.5 mL of appropriate growth medium and incubated for 5 h, so that a dense monolayer (70-80% confluent) could be obtained, at the end of the experiment. After incubation, 0.5 mL of growth medium containing different concentrations of CNDs was added to each well. Cells incubated in the absence of CNDs were taken as control. In all cases, three parallel samples were prepared for each tested concentration (including control). After incubating for 24 h (short-term viability assay) or 48 h (long-term viability assay), the culture supernatant was removed and the dead cells were washed off with PBS. Afterwards, adherent cells were stained and fixed to the bottom of the plate by adding 200 μL of crystal violet solution and incubating for 30 min, at room temperature. The excess crystal violet solution was removed by submerging the plates in DDW. Thereupon, the plates were allowed to air-dry and the cells were destained twice, by adding 1 mL of methanol and incubating for 20 min.[2] Finally, the optical absorbance was measured at 570 nm and the % cell viability was calculated using the formula:

$$\%\ cell\ viability\ =\ (OD\ treated/OD\ non-treated)*100$$

where % cell viability represents the amount of alive cells, OD non-treated = absorbance in control wells and OD treated = absorbance at different concentrations of CNDs.

Trypan blue assay

Cells were seeded in 24-well plates and incubated for 5 h, as mentioned above. The CNDs were then added to the cells and further incubated for 24 or 48 h. The cells in the supernatant and the adherent cells (with trypsin) were collected and washed twice with PBS. Next, cells were stained with trypan blue solution for 5 min. The live and dead cells were counted using a hemocytometer.[3]

Cell cycle analysis

For cell cycle analysis, HEK-293 cells were firstly synchronized with serum starvation. After serum starvation for 20 h, a high percentage of the cells were inhibited at G0/G1 phase. Cells were then trypsinized and seeded in 24-well plates, as mentioned before and restimulated to enter cell cycle in the presence of 10% FBS for

24 h, prior treatment with CNDs.[4] After 24 h of incubation, CNDs (200 and 800 μg mL^{-1}) were added to the cells and further incubated for 24 h. Then, the supernatant was removed and cells were trypsinized, collected and centrifuged at 2200 rpm, for 6 min. The cell pellet was washed with PBS and centrifuged under the same conditions. The washing step was repeated once more. After removal of the PBS, cells were fixed by adding to the cell pellet 4 mL of 70% (v/v) cold ethanol dropwise, under vortex shaking. Cells were stored at 4°C until measurement. Prior to flow cytometry, cells were subjected to centrifugation (2200 rpm, for 6 min) to remove ethanol and the resulting cell pellet was washed twice with PBS, according to the above mentioned procedure. The cell pellet was resuspended in solutions of propidium iodide (final concentration: 50 μg mL^{-1}) and Ribonuclease type A (final concentration: 100 μg mL^{-1}) and were kept in the dark, for 45 min, at 37°C, before transferred to special tubes for flow cytometry analysis.[5] The experiment was conducted in triplicate and the differences were plotted as error bars. A minimum of 30,000 events were recorded for each analysis. The proportion of cells in the G0/G1, S, and G2/M phase of the cell cycle was calculated from the resulting DNA histograms.

Cellular imaging

Cell imaging was performed according to our previous studies.[1, 6] In brief, HeLa, A549, MDA-MB-231 and HEK-293 cells were seeded on 22×22 mm glass cover-slips and placed inside a 6-well plate. Each cell line was incubated for 5 h in 1 mL of appropriate medium, under the conditions described above. Afterwards, 1 mL of fresh medium containing 200 μg mL^{-1} of CNDs was added to each well of a chamber slide and further incubated for 2 h. Prior to observation, cells were washed three times with PBS.

Scratch assay

Cells at a density of 4×10^4 cells/well were seeded into 24-well plates, using an appropriate growth medium, so as to produce a nearly confluent cell monolayer. An elongated scratch was subsequently generated, using a sterile 200 μL tip on the monolayer in each well. Wells were washed with PBS to remove cell debris. Serum-free RPMI medium was used as negative control; RPMI medium with 8% FBS was used as positive control (selected after evaluating cell migration with various

concentrations of FBS, ranging between 1 and 10%). Cells incubated with 0.3% FBS were selected as control, since this concentration was found to be adequate for cells to migrate, but inadequate to promote cell proliferation. The CNDs were tested at a final concentration of 200 μg mL^{-1} in a medium containing 0.3% FBS. The distance of the gap was observed under microscope, at the same three positions for each gap, for two different time periods (i.e. 24 and 48 h post-treatment) to evidence the repair process for control and CNDs-treated cells. Images were captured at a 4 × magnification using a digital camera mounted on a microscope and they were further analyzed using COREL DRAW X6 software.[7] The migration of cells toward scratch was expressed as % percentage of wound closure:

$$Wound\ closure\ (\%) = \frac{ADBC_0 - ASBC_t}{ADBC_0} \times 100$$

where *ADBC* stands for the average distance between scratch at time 0 ($ADBC_0$) and at different time points ($ADBC_t$).

Blood clot time

To assess blood clot time in the presence of CNDs, whole blood from healthy volunteers was collected and incubated on clean glass slides, in the presence of CNDs (0.1-1.0 mg mL^{-1}). After the addition of 25 μL of $CaCl_2$ (50 mM) to each sample, the time needed to observe the first visible clot sign was recorded. Normal saline (control) was used instead of CNDs, for comparison.[8]

Hemolysis assay

For the hemolysis assay, human blood samples were collected from healthy volunteers, who did not undergo any medication. Trisodium citrate was added as anticoagulant and blood was used without further treatment. Dispersions of CNDs in normal saline were prepared at concentration of CNDs between 0.1 and 1.0 mg mL^{-1} and were tested according to a previous report.[9]

Stability of CNDs solution

The synthesized CNDs exhibit stable fluorescence over the wide range of 4.0-9.0; more acidic (pH < 4.0) or alkaline conditions (pH > 9.0) cause a dramatic decrease to the fluorescence intensity. The alterations in the fluorescence intensity can be justified by the variations in the deprotonation degree of the surface atoms of CNDs.[10] The

effect of ionic strength was also examined by adding NaCl and Na_2SO_4, separately, at concentrations up to 1 mol L^{-1}. The results showed that the CNDs exhibit stable fluorescence, despite the increase in ionic strength. As regards the photobleaching of the CNDs, relevant experiments revealed that the fluorescence of CNDs, irradiated with a 150 W Xe lamp for 2 h was stable, bespeaking excellent photostability. Finally, aqueous solutions of the CNDs, stored at room temperature, were found to emit unaltered fluorescence for five days (reduction of fluorescence < 3%). According to the aforementioned results, it can be concluded that the synthesized CNDs exhibit excellent photostability, making them suitable for a wide range of applications.

Cr(VI) detection-Analytical figures of merit

Linear response was achieved between 1.7 and 67.5 nM, with a coefficient of determination (R^2) of 0.9981. The limit of detection, defined as a signal-to-noise ratio = 3, was calculated to be 0.3 nM. The relative standard deviations (% RSD) of intra-day and inter-day measurements (repeatability and reproducibility) were 1.9 and 2.5%, respectively. As a proof-of-concept, the applicability of the developed method was tested by analyzing environmental water samples (lake, river and sea water) and by performing recovery experiments. Highly satisfactory recoveries were achieved, ranging between 95.0 and 99.2% in all samples.

FRET mechanism exploration

The contribution of the fluorescence resonance energy transfer (FRET) phenomenon was examined. The criteria that need to be met according to Förster's nonradioactive energy transfer theory are: (a) the ability of the donor to produce fluorescence light, (b) there is an overlap between the fluorescence emission spectrum of the donor and the UV absorption spectrum of the acceptor and (c) the distance between the donor and the acceptor is lower than 8 nm.[11] In our case, the first two criteria are met, so the examination of the third criterion was necessary. To do so, the following equations were used:

$$E = 1 - \frac{F}{F_0} = \frac{R_0^6}{R_0^6 + r^6}$$

$$R_0^6 = 8.79 \times 10^{-25} K^2 n^{-4} \Phi J$$

$$J(\lambda) = \int_0^\infty F_D(\lambda)\varepsilon_A(\lambda)\lambda^4 d\lambda = \frac{\int_0^\infty F_D(\lambda)\varepsilon_A(\lambda)\lambda^4 d\lambda}{\int_0^\infty F_D(\lambda) d\lambda}$$

where, E is the efficiency of energy transfer between the donor and the acceptor, R_0 is the critical distance at which transfer efficiency equals 50%, r is the distance between a donor and an acceptor, K^2 stands for the orientation factor related to the geometry of the donor-acceptor dipole (=2/3), n is the refractive index of the medium (=1.33); φ is the fluorescence quantum yield of the donor (=0.514), J expresses the degree of spectral overlap of the emission of the donor (i.e. CNDs) and the absorption of the acceptor (i.e. Cr(VI) at neutral pH), $F_D(\lambda)$ is the corrected fluorescence intensity of the donor at wavelength λ and $\varepsilon(\lambda)$ is the molar absorption coefficient of the acceptor at wavelength λ. The distance (r) between the donor and the acceptor was found to be 16.6 nm, which is higher than the accepted distance of 8 nm.

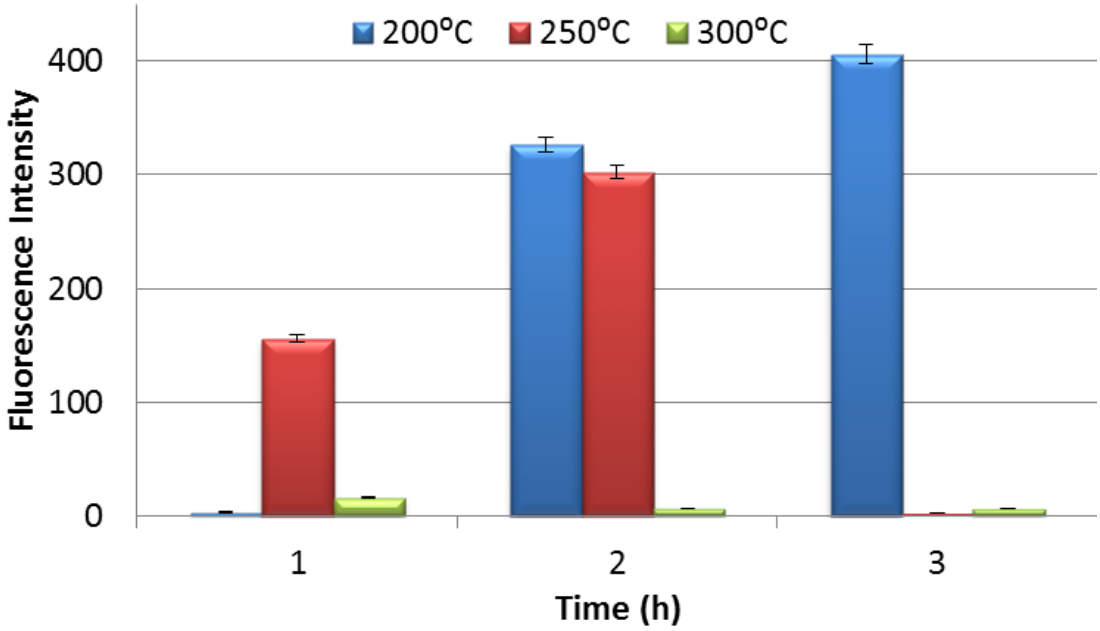

Figure S1: Fluorescence intensity at λ_{ex} /λ_{em}: 330/380 nm of the CNDs from different carbonization temperature and time combinations.

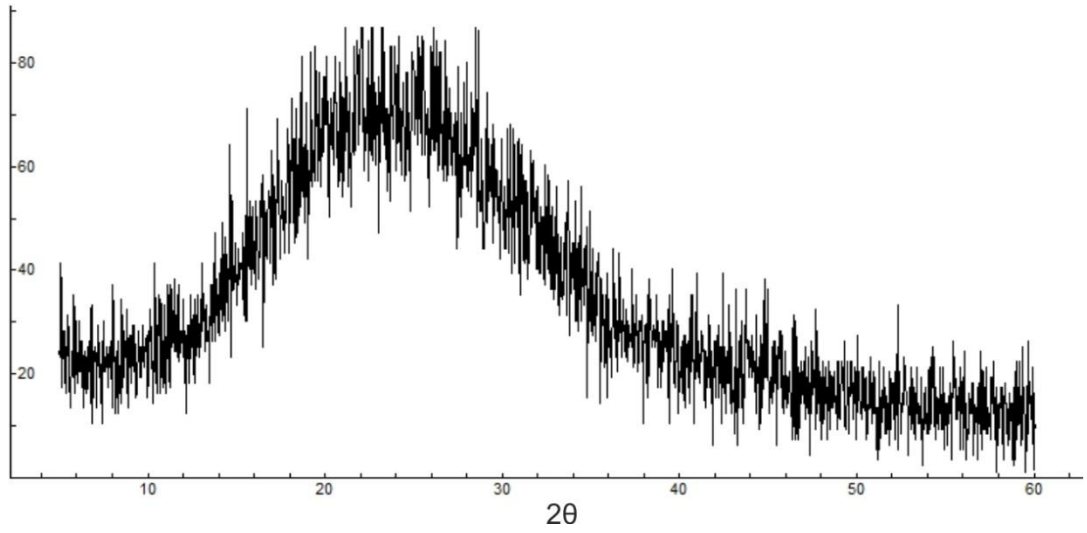

Figure S2: XRD diffractogram of the synthesized CNDs.

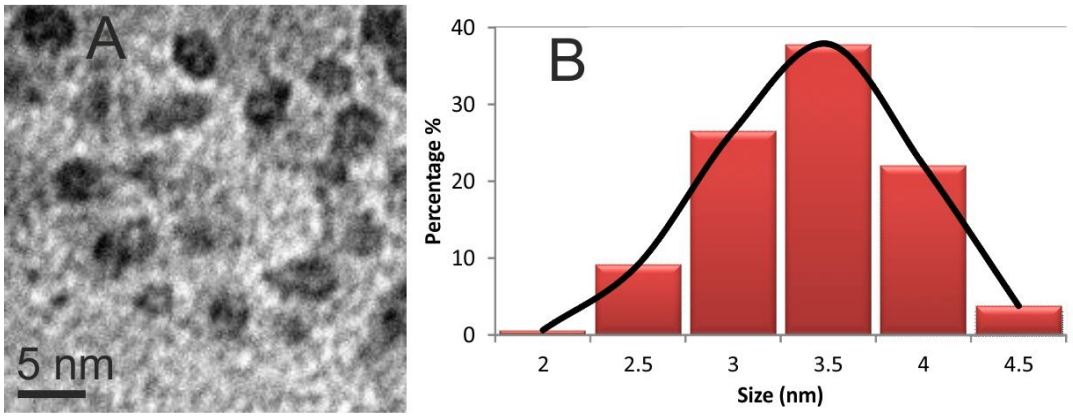

Figure S3: (A) TEM image and (B) size distribution of CNDs from carbonization of human nails.

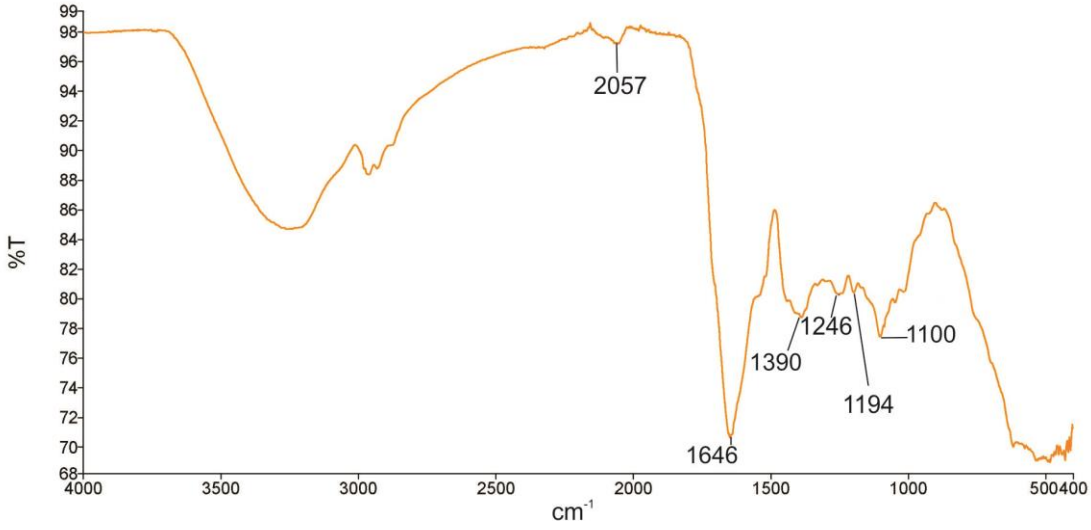

Figure S4: FTIR spectrum of CNDs.

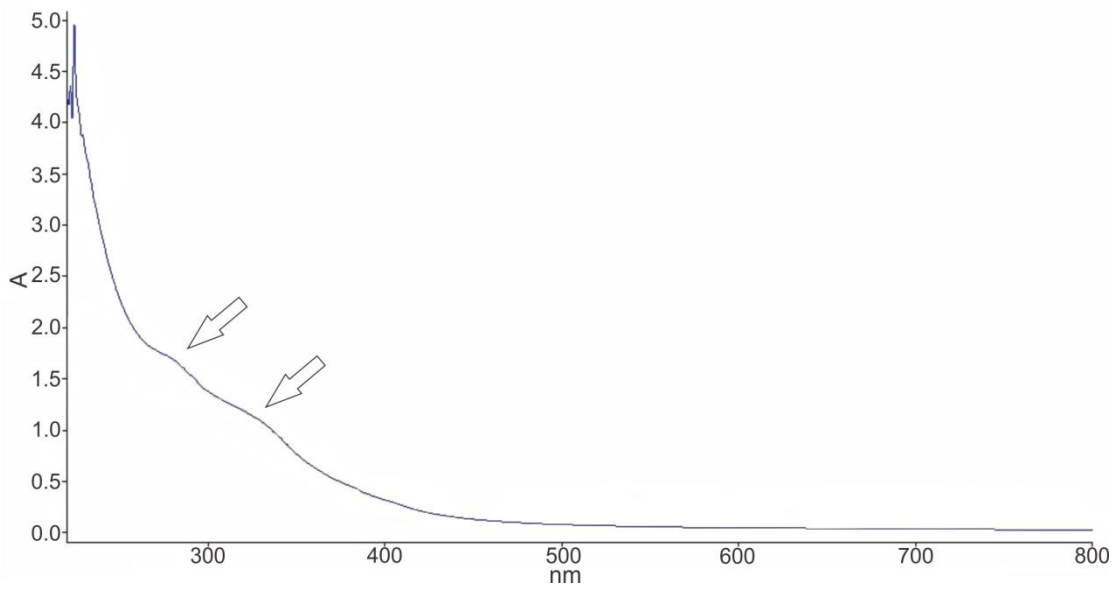

Figure S5: UV-Vis spectrum of the synthesized CNDs.

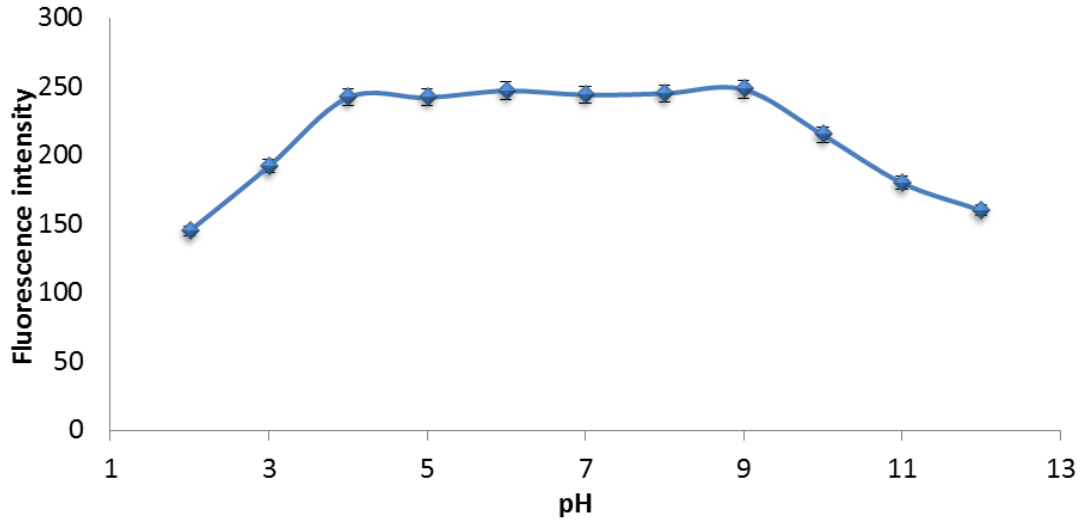

Figure S6: Fluorescence intensity of the CNDs in relation to the pH of an aqueous dispersion.

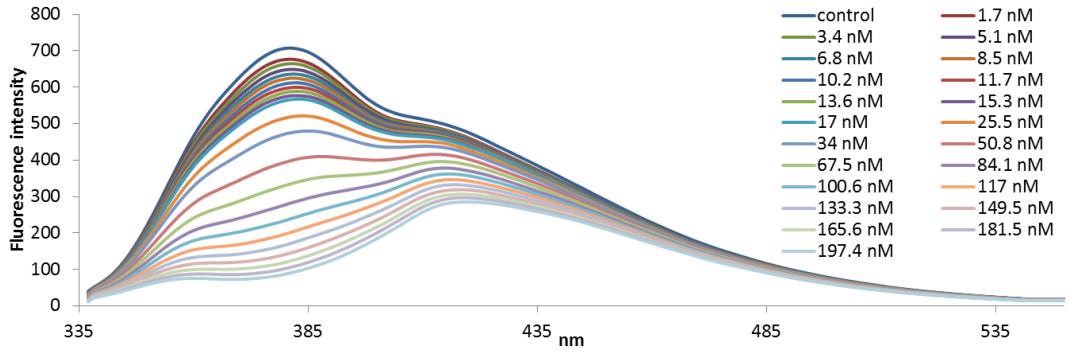

Figure S7: Fluorescence emission spectra of the CNDs in the absence and in the presence of Cr(VI) up to 181.5 nM.

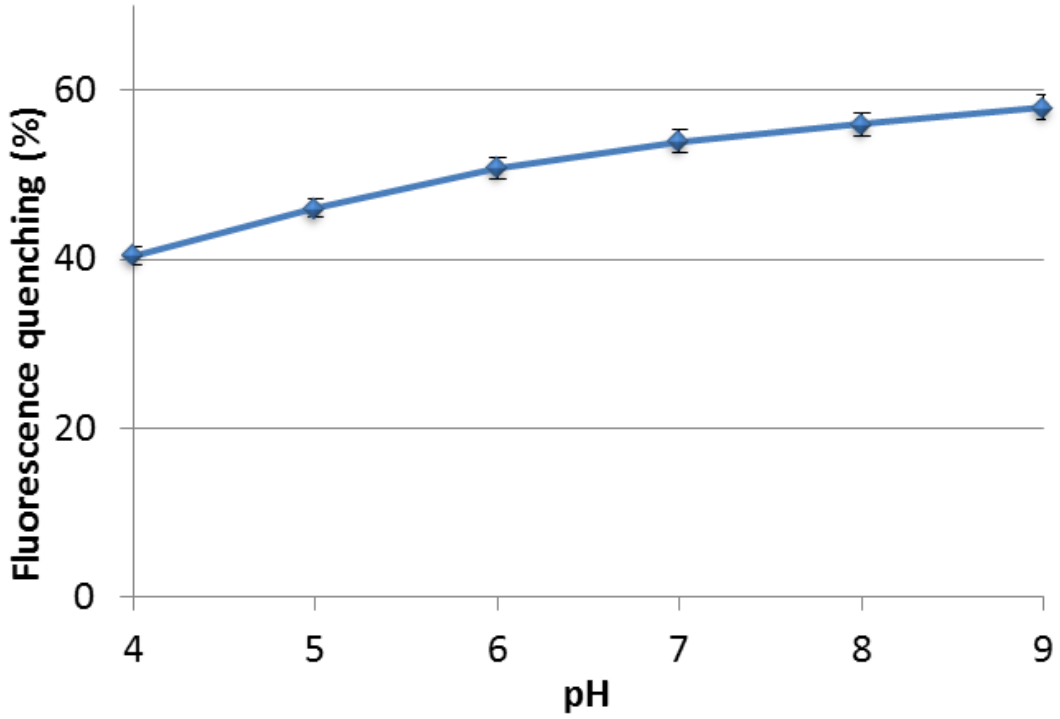

Figure S8: Quenching of the CNDs emitted fluorescence in relation to the pH of a solution.

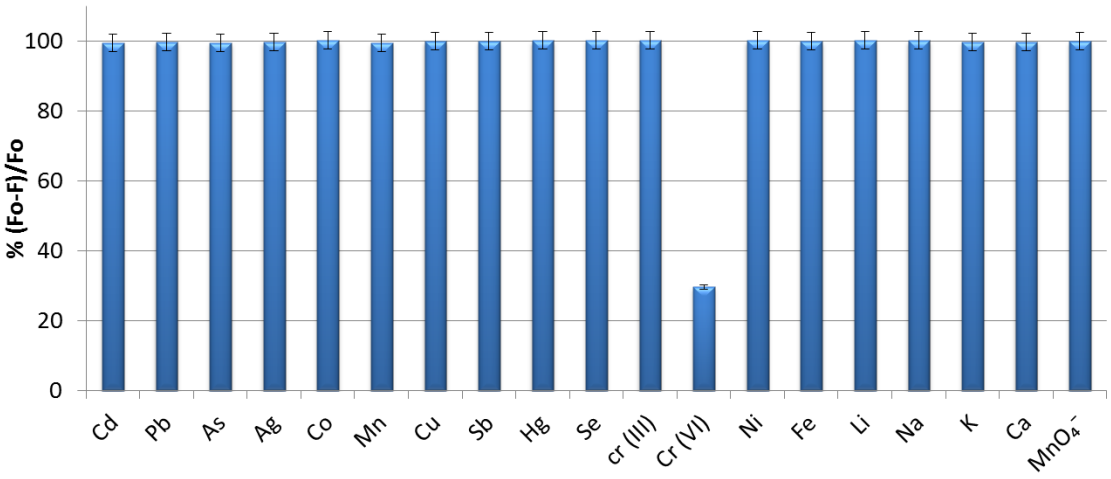

Figure S9: Fluorescence quenching caused by 100 nM various metal ions.

Table S1: Analysis of environmental water samples and recoveries after spiking.

Sample	Added (nM)	Measured (nM)	Recovery (%)
Lake water	0	0	-
	5.0	4.85	97.0
	25.0	24.8	99.2
river water	0	0	-
	5.0	4.9	98.0
	25.0	24.7	98.8
sea water	0	0	-
	5.0	4.75	95.0
	25.0	24.5	98.0

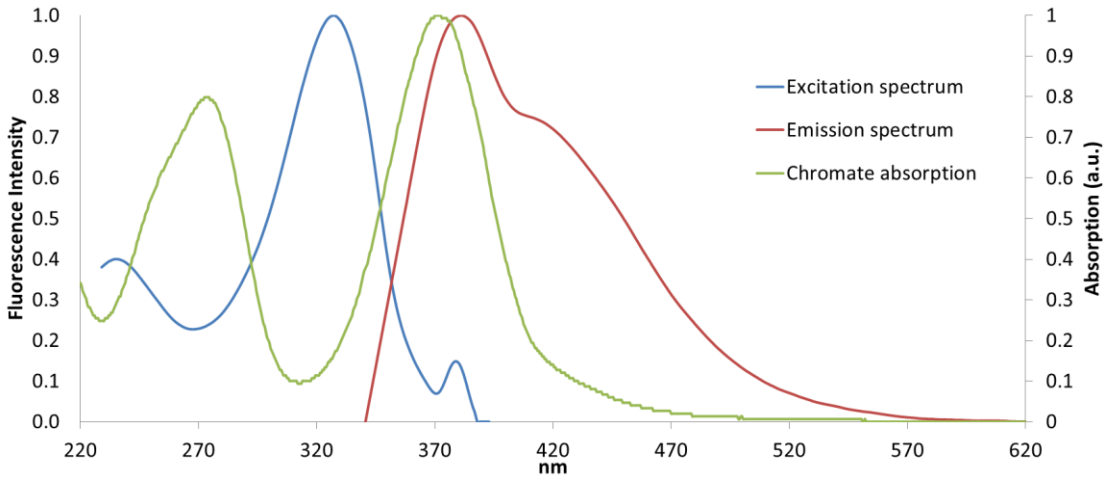

Figure S10: Normalized excitation and emission spectra of the CNDs and normalized absorption spectrum of Cr(VI).

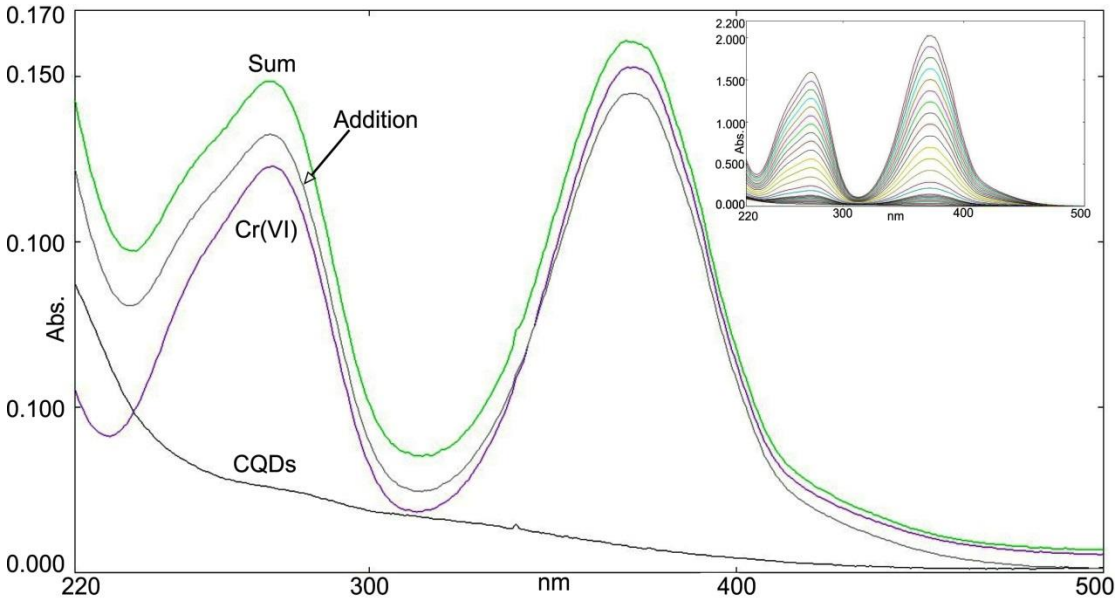

Figure S11: UV-VIS absorption spectra of CNDs, Cr(VI), their mixture and the sum of the first two spectra (inset: consecutive additions of Cr(VI) to a CNDs dispersion)

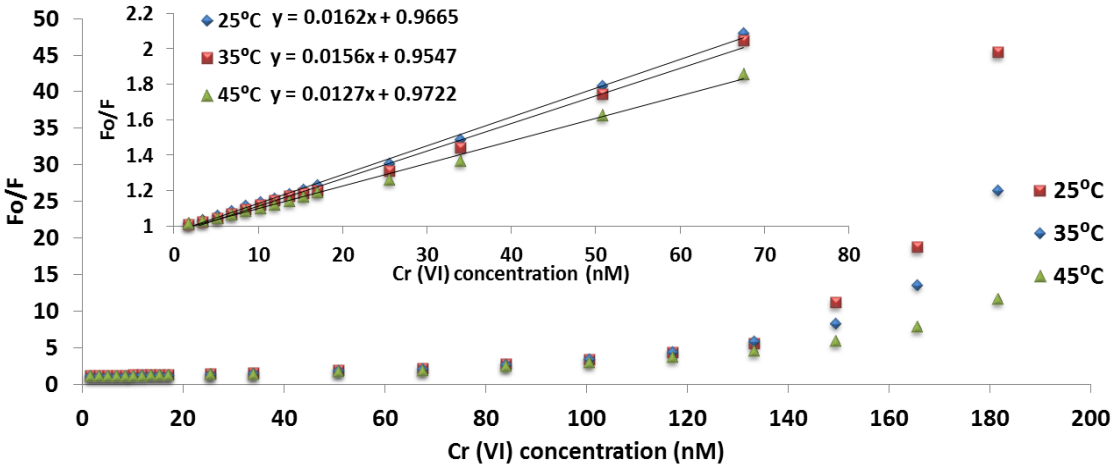

Figure S12: Stern-Volmer plots of the developed fluorescent sensor in three different temperatures, inset: linear range of the three Stern-Volmer plots.

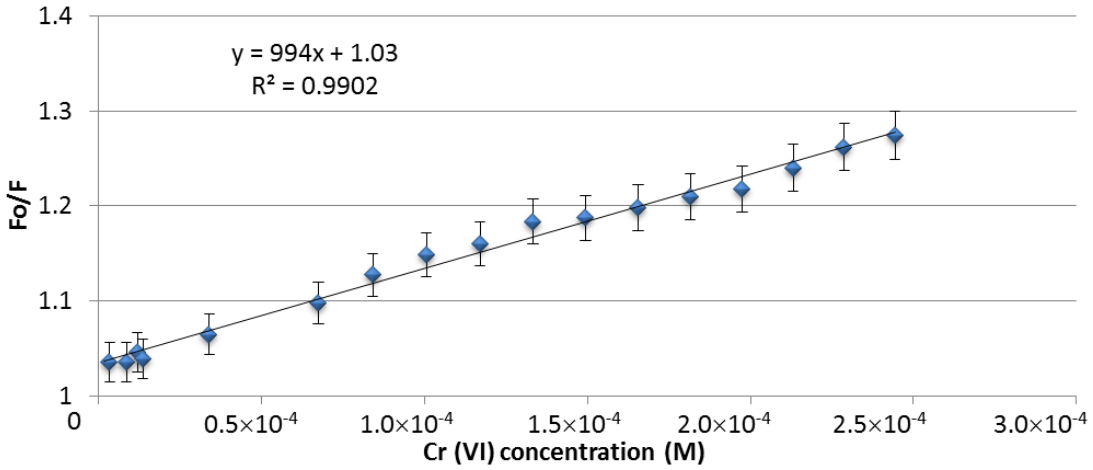

Figure S13: Fitted Stern-Volmer plot for CNDs-Cr(VI) after correction for inner filter effect.

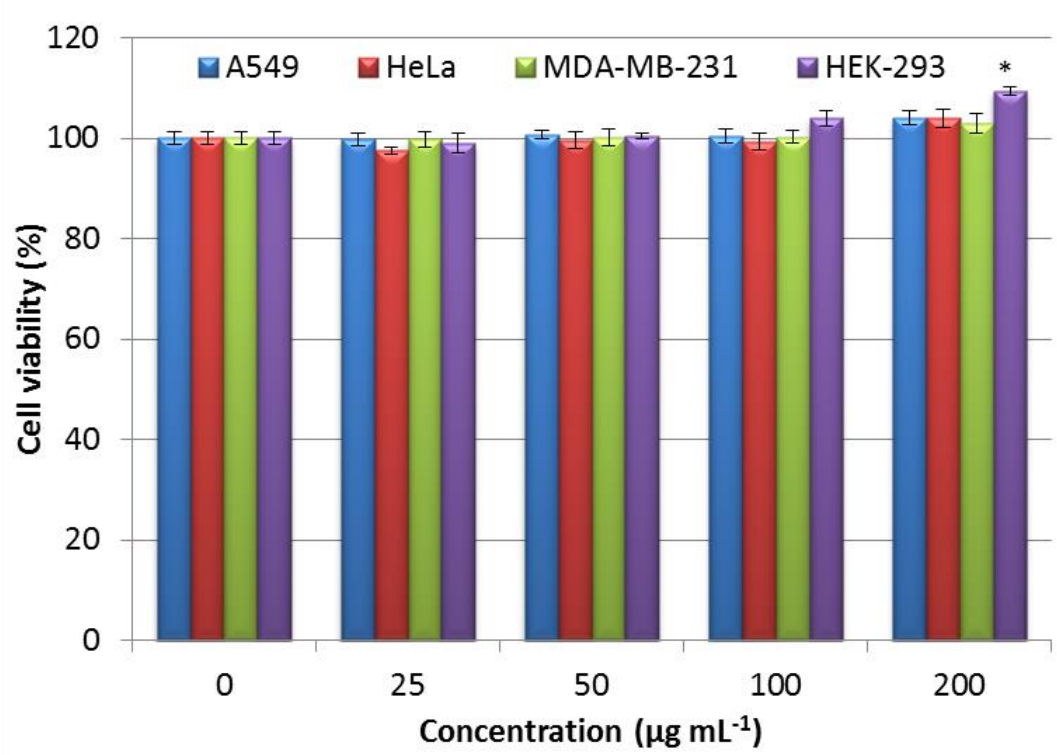

Figure S14: Cell viability of four epithelial cell lines after incubation with various concentration of CNDs up to 200 µg L^{-1}, for 24 h (statistically significant differences at $p<0.05$ are denoted with *).

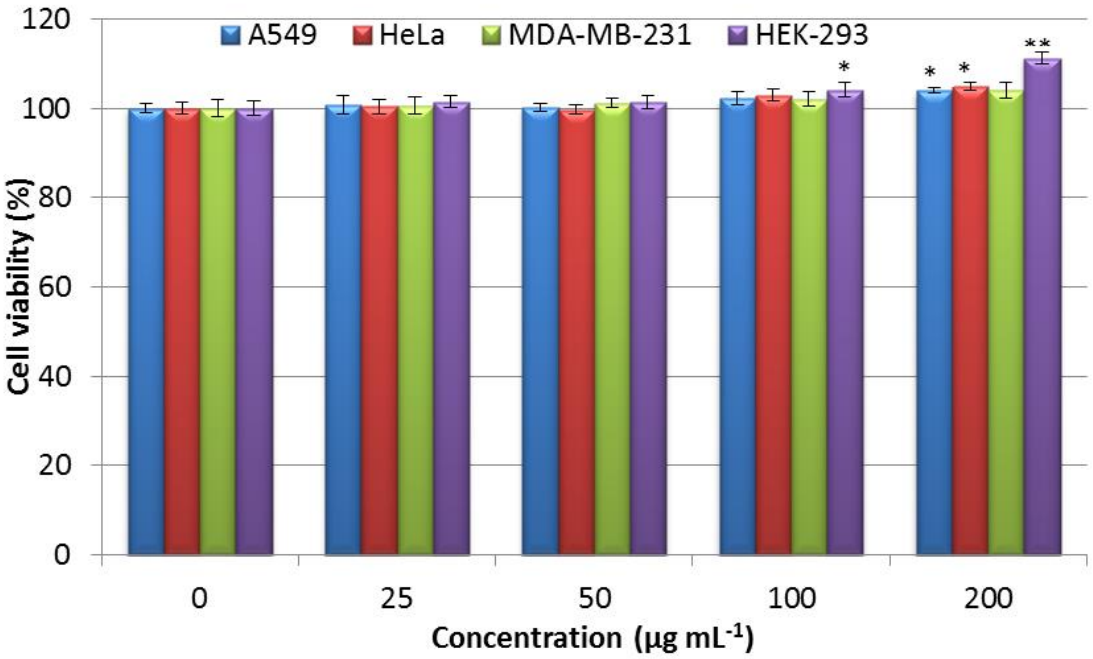

Figure S15: Cell viability of four epithelial cell lines after incubation with various concentration of CNDs up to 200 µg L^{-1}, for 48 h (statistically significant differences at $p<0.05$ and $p<0.01$ are denoted with * and **, respectively).

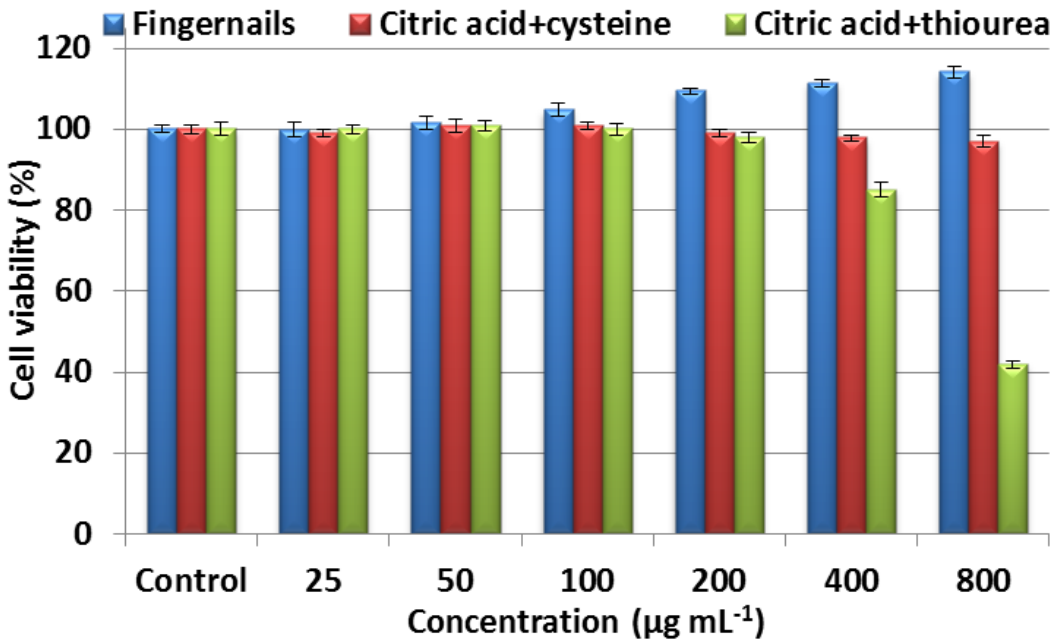

Figure S16: Cell viability of HEK-293 cells after incubation for 24 h with different concentrations of CNDs, derived from carbonization of human fingernails, citric acid and cysteine and citric acid and thiourea.

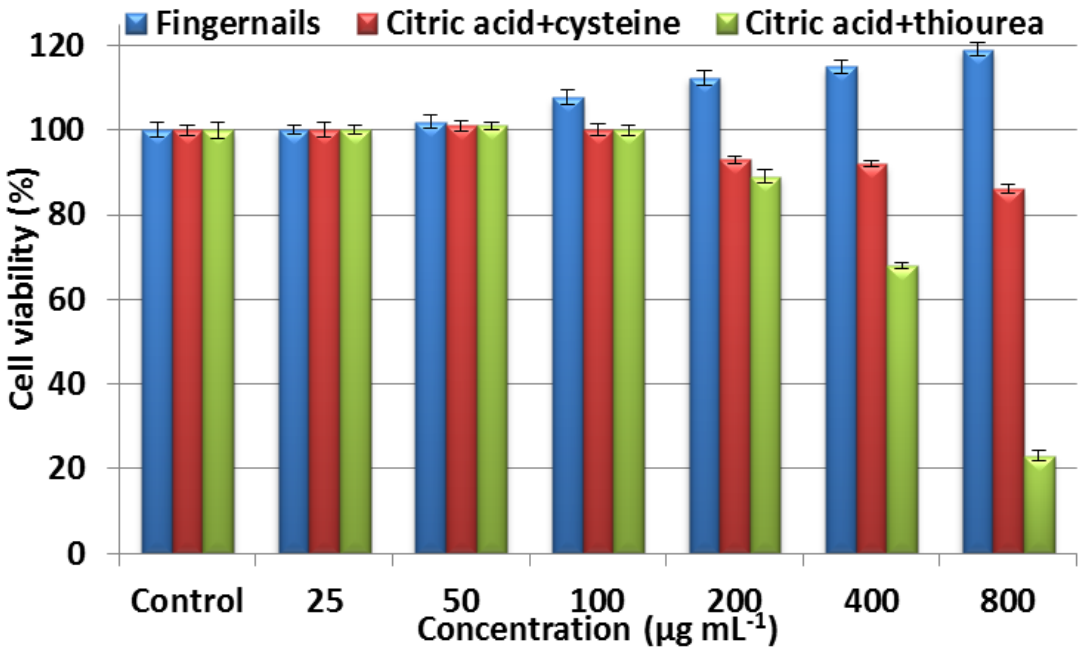

Figure S17: Cell viability of HEK-293 cells after incubation for 48 h with different concentrations of CNDs, derived from carbonization of human fingernails, citric acid and cysteine and citric acid and thiourea.

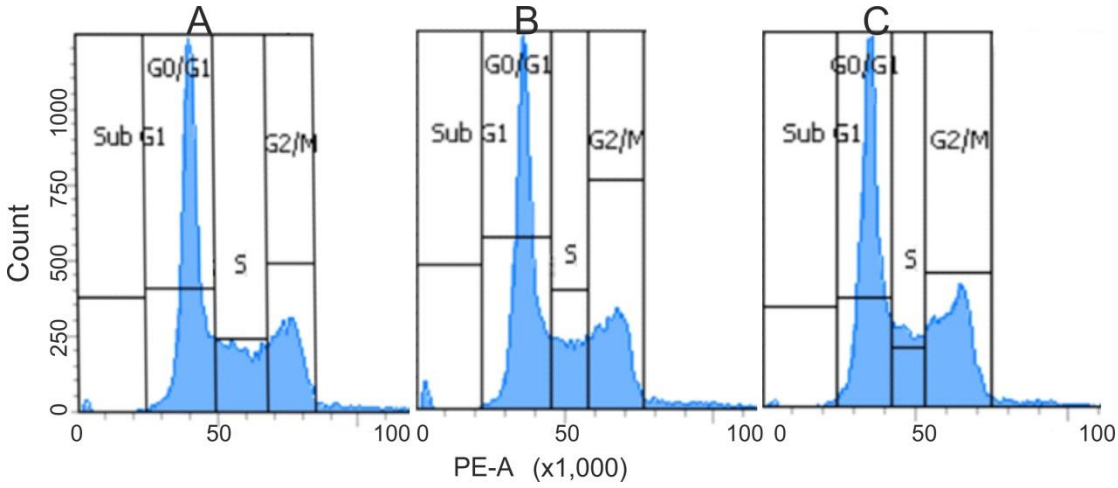

Figure S18: DNA histograms of (a) control HEK-293 cells and after 24 h of incubation with (b) 200 and (c) 800 µg $L^{-1}$of CNDs.

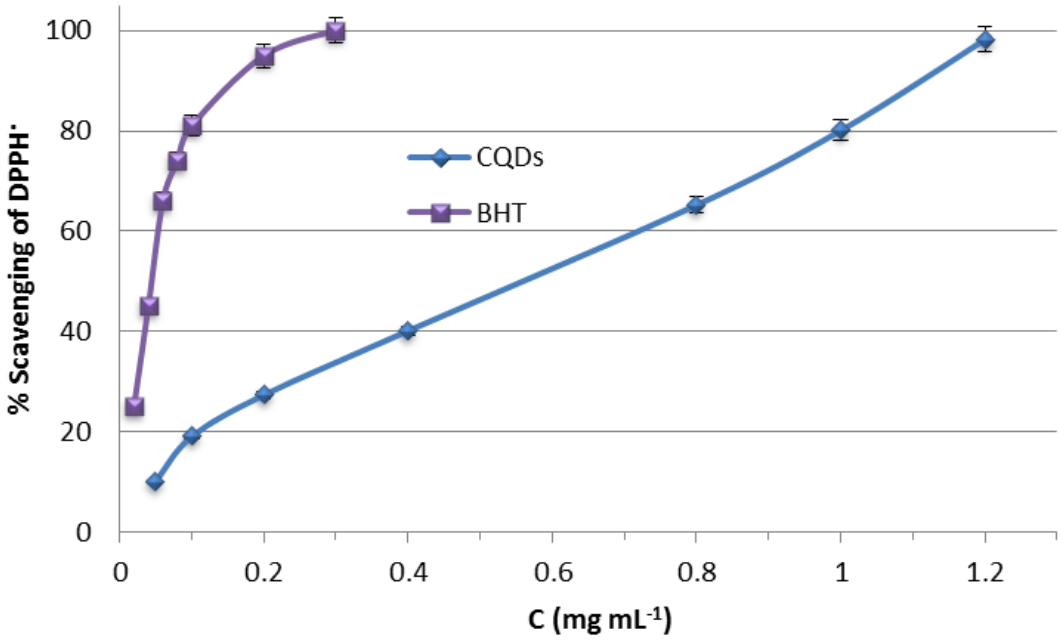

Figure S19: Scavenging activity of the synthesized CNDs and BHT for the DPPH free radical.

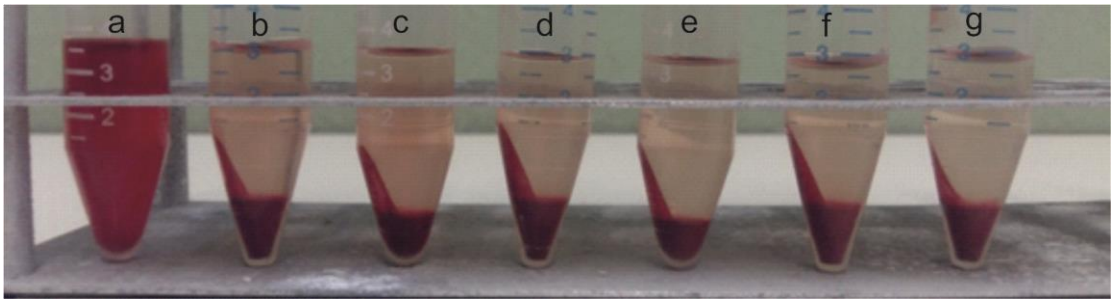

Figure S20: Whole blood samples incubated with Triton-X (a), CNDs at 100 (b), 200 (c), 400 (d), 800 (e), 1000 (f) μg L^{-1} and normal saline (g).

Table S2: Comparison of the developed probe for Cr(VI) detection, with other CNDs-based fluorescent probes

carbon source	$\lambda_{ex}/\lambda_{em}$ (nm)	QY (compared to quinine sulfate)	matrix	recoveries (%)	LOD (μM)	linear range (μM)	reference
Pineapple juice	370/453	10.06	-	-	0.052	1-18	[12]
degrease cotton	355/440	10.2	water, soil	94.15-99.20	120/190	1000-6000	[13]
citric acid and cystamine dihydrochloride	420/478	39.7	-	-	0.86	1-80	[14]
1,2-ethylenediamine and glucose	403/502	9.6	-	-	0.023	1.5-30	[15]
Ammonium citrate	350/439	20.05	-	-	0.01	0-50	[16]
1-(2-Pyridylazo)-2-naphthol	370/430	6.2	tap water, fish	83.69-106.96	1.17	5-125	[17]
pomelo	380/450	18.7	tap and lake water	92-107	0.52	0-40	[18]
glutathione	394/585	2.1	tap, mineral and lake water	94.9-102.8	1.5	0-45	[19]
glucose	360/450	7.6	-	-	0.02	0-0.2	[20]
cysteine	390/460	18.1	lake water	-	0.0014	0.5	[21]

citric acid and diethylenetriamine	360/450	88.6[1]	-	-	-	0.01-50	[22]
citric acid and reduced glutathione	370/440	69.4	water and soil	90-107	0.03	0.10-12	[23]
dopamine, citric acid and ammonium persulfate	331/495	93[2]	-	-	1×10^{-11} M	2×10^{-11} to 3×10^{-10} M	[24]
Human fingernails	330/380	81.4	lake, river, sea water	95.0-99.2	0.0003	1.7 - 67.5 nM	This work

[1]referenced to cumarin 1
[2]referenced to rhodamine B

References

(1) Chatzimitakos, T.; Kasouni, A.; Sygellou, L.; Avgeropoulos, A.; Troganis, A.; Stalikas, C. Two of a Kind but Different: Luminescent Carbon Quantum Dots from Citrus Peels for Iron and Tartrazine Sensing and Cell Imaging. *Talanta* **2017,** *175*, 305-312.
(2) Feoktistova, M.; Geserick, P.; Leverkus, M. Crystal Violet Assay for Determining Viability of Cultured Cells. *Cold Spring Harbor Protocols* **2016,** *2016*, pdb.prot087379.
(3) Strober, W. Trypan Blue Exclusion Test of Cell Viability. In *Current Protocols in Immunology*; John Wiley & Sons, Inc.: 2001.
(4) Chen, M.; Huang, J.; Yang, X.; Liu, B.; Zhang, W.; Huang, L.; Deng, F.; Ma, J.; Bai, Y.; Lu, R.; Huang, B.; Gao, Q.; Zhuo, Y.; Ge, J. Serum Starvation Induced Cell Cycle Synchronization Facilitates Human Somatic Cells Reprogramming. *PLOS ONE* **2012,** *7*, e28203.
(5) Pozarowski, P.; Darzynkiewicz, Z. Analysis of Cell Cycle by Flow Cytometry. In *Checkpoint Controls and Cancer: Volume 2: Activation and Regulation Protocols*; Schönthal, A. H., Ed.; Humana Press: Totowa, NJ, 2004; pp 301-311.
(6) Chatzimarkou, A.; Chatzimitakos, T. G.; Kasouni, A.; Sygellou, L.; Avgeropoulos, A.; Stalikas, C. D. Selective FRET-Based Sensing of 4-Nitrophenol and Cell Imaging Capitalizing on the Fluorescent Properties of Carbon Nanodots from Apple Seeds. *Sens. Actuators, B* **2018,** *258*, 1152-1160.
(7) Ko, M. H.; Li, C. Y.; Lee, C. F.; Chang, C. K.; Fang, S. H. Scratch Wound Closure of Myoblasts and Myotubes is Reduced by Inflammatory Mediators. *International Wound Journal* **2016,** *13*, 680-685.
(8) Durgadas, C. V.; Sreenivasan, K.; Sharma, C. P. Bright Blue Emitting CuSe/ZnS/Silica Core/Shell/Shell Quantum Dots and their Biocompatibility. *Biomaterials* **2012,** *33*, 6420-6429.
(9) Bankoti, K.; Rameshbabu, A. P.; Datta, S.; Das, B.; Mitra, A.; Dhara, S. Onion Derived Carbon Nanodots for Live Cell Imaging and Accelerated Skin Wound Healing. *J. Mater. Chem. B* **2017,** *5*, 6579-6592.
(10) Shi, B.; Zhang, L.; Lan, C.; Zhao, J.; Su, Y.; Zhao, S. One-Pot Green Synthesis of Oxygen-Rich Nitrogen-Doped Graphene Quantum Dots and their Potential Application in pH-Sensitive Photoluminescence and Detection of Mercury(II) Ions. *Talanta* **2015,** *142*, 131-139.
(11) Pan, X.; Qin, P.; Liu, R.; Wang, J. Characterizing the Interaction between Tartrazine and Two Serum Albumins by a Hybrid Spectroscopic Approach. *J. Agric. Food Chem.* **2011,** *59*, 6650-6656.
(12) Sharma, S.; Umar, A.; Mehta, S. K.; Kansal, S. K. Fluorescent Spongy Carbon Nanoglobules Derived from Pineapple Juice: A Potential Sensing Probe for Specific and Selective Detection of Chromium (VI) Ions. *Ceram. Int.* **2017,** *43*, 7011-7019.
(13) Wang, J.; Qiu, F.; Li, X.; Wu, H.; Xu, J.; Niu, X.; Pan, J.; Zhang, T.; Yang, D. A Facile One-Pot Synthesis of Fluorescent Carbon Dots from Degrease Cotton for the Selective Determination of Chromium Ions in Water and Soil Samples. *J. Lumin.* **2017,** *188*, 230-237.
(14) Chen, J.; Liu, J.; Li, J.; Xu, L.; Qiao, Y. One-Pot Synthesis of Nitrogen and Sulfur Co-Doped Carbon Dots and its Application for Sensor and Multicolor Cellular Imaging. *J. Colloid Interface Sci.* **2017,** *485* (Supplement C), 167-174.
(15) Gong, X.; Liu, Y.; Yang, Z.; Shuang, S.; Zhang, Z.; Dong, C. An "On-Off-On" Fluorescent Nanoprobe for Recognition of Chromium(VI) and Ascorbic Acid Based

on Phosphorus/Nitrogen Dual-Doped Carbon Quantum Dot. *Anal. Chim. Acta* **2017,** *968* (Supplement C), 85-96.
(16) Fang, L.; Zhang, L.; Chen, Z.; Zhu, C.; Liu, J.; Zheng, J. Ammonium Citrate Derived Carbon Quantum Dot as On-Off-On Fluorescent Sensor for Detection of Chromium(VI) and Sulfites. *Mater. Lett.* **2017,** *191* (Supplement C), 1-4.
(17) Zhang, H.-Y.; Wang, Y.; Xiao, S.; Wang, H.; Wang, J.-H.; Feng, L. Rapid Detection of Cr(VI) Ions Based on Cobalt(II)-Doped Carbon Dots. *Biosens. Bioelectron.* **2017,** *87*, 46-52.
(18) Shen, J.; Shang, S.; Chen, X.; Wang, D.; Cai, Y. Highly Fluorescent N, S-Co-Doped Carbon Dots and their Potential Applications as Antioxidants and Sensitive Probes for Cr (VI) Detection. *Sens. Actuators, B* **2017,** *248* (Supplement C), 92-100.
(19) Kong, L.; Chu, X.; Liu, W.; Yao, Y.; Zhu, P.; Ling, X. Glutathione-Directed Synthesis of Cr(vi)- and Temperature-Responsive Fluorescent Copper Nanoclusters and their Applications in Cellular Imaging. *New J. Chem.* **2016,** *40*, 4744-4750.
(20) Xu, Z.; Wang, C.; Jiang, K.; Lin, H.; Huang, Y.; Zhang, C. Microwave-Assisted Rapid Synthesis of Amphibious Yellow Fluorescent Carbon Dots as a Colorimetric Nanosensor for Cr(VI). *Part. Part. Syst. Charact.* **2015,** *32*, 1058-1062.
(21) Xiao, D.; Pan, R.; Li, S.; He, J.; Qi, M.; Kong, S.; Gu, Y.; Lin, R.; He, H. Porous Carbon Quantum Dots: One Step Green Synthesis via L-Cysteine and Applications in Metal Ion Detection. *RSC Adv.* **2015,** *5*, 2039-2046.
(22) Zheng, M.; Xie, Z.; Qu, D.; Li, D.; Du, P.; Jing, X.; Sun, Z. On–Off–On Fluorescent Carbon Dot Nanosensor for Recognition of Chromium(VI) and Ascorbic Acid Based on the Inner Filter Effect. *ACS Appl. Mater. Interfaces* **2013,** *5*, 13242-13247.
(23) Vaz, R.; Bettini, J.; Júnior, J. G. F.; Lima, E. D. S.; Botero, W. G.; Santos, J. C. C.; Schiavon, M. A. High Luminescent Carbon Dots as an Eco-Friendly Fluorescence Sensor for Cr(VI) Determination in Water and Soil Samples. *J. Photochem. Photobiol., A* **2017,** *346*, 502-511.
(24) Zhao, S.; Song, X.; Bu, X.; Zhu, C.; Wang, G.; Liao, F.; Yang, S.; Wang, M. Polydopamine Dots as an Ultrasensitive Fluorescent Probe Switch for Cr(VI) in vitro. *J. Appl. Polym. Sci.* **2017,** *134*, 44784.